Identification of cost-effective multihazard capacity of nuclear power plant using multi-objective genetic algorithm

Eujeong Choi
Senior Researcher, Structural and Seismic Safety Research Division, Korea Atomic Energy Research Institute (KAERI), Daejeon, 34057, Republic of Korea.

Shinyoung Kwag
Associate Professor, Department of Civil and Environmental Engineering, Hanbat National University, Daejeon, 34158, Republic of Korea

Daegi Hahm
Principal Researcher, Structural and Seismic Safety Research Division, Korea Atomic Energy Research Institute (KAERI), Daejeon, 34057, Republic of Korea.

ABSTRACT: After the Tohoku earthquake-tsunami (Japan, 2011), the regulatory efforts to mitigate the external hazards increase both safety requirements and the total capital cost of nuclear power plant (NPP). In these circumstances, identify not only the robust but also the cost-effective capacity of NPP becomes one of the most important tasks for the nuclear power industry. A few studies performed to relocate the seismic capacity of NPP, yet the effect of multihazard had not been accounted for NPP capacity optimization. The major challenges in extending this problem to the multihazard dimension are (1) high computational cost for both multihazard risk quantification and system-level optimization and (2) lack of capital cost database of NPP. To resolve these issues, this paper presents an effective method that identifies the optimal multihazard capacity of NPP using a multi-objective genetic algorithm, two-stage direct quantification of fault tree using Monte Carlo simulation (two-stage DQFM) method, and indirect capital cost measure. The proposed multihazard capacity optimization framework for NPP is demonstrated and tested by the NPP example.

1. INTRODUCTION

An NPP is one of the most robust man-made structure systems which ensures a sufficient safety margin through regular probabilistic safety assessments (PSAs). However, NPP PSA is mainly performed for single hazards risk (e.g., Seismic PSA) while an NPP system can be exposed to the joint effect of various multihazard, which consist of more than one hazard. In these circumstances, an NPP system which robust against the various type of single hazards can remain vulnerable to multihazard since securing the NPP system from a single hazard does not necessarily guarantee the multihazard safety of the NPP (Choi *et al*., 2020). For example, Fukushima-Daiichi NPP which experienced a core-damage accident due to the earthquake-tsunami (Japan, 2011), was robust enough from a seismic safety perspective yet prone to the joint effect of strong ground motion and extreme flooding. Therefore, mitigating the risk from a multihazard perspective is one of the top priorities of the nuclear power industry. At the same time, not only the multihazard safety of NPP but also reducing the capital cost of the NPP, which is often proportional to the capacity of the structure, systems, and components (SSCs), become a critical issue in making cost-competitive commercial nuclear energy.

However, despite the importance of these two issues, cost and multihazard risk-informed design or maintenance had not been extensively investigated in the field of nuclear safety engineering. Therefore, we aim to identify the

optimal relocation of multihazard capacity SSCs of NPP which minimize both multihazard risk and capital cost.

To date, in the field of structure and system reliability engineering, various frameworks were developed to identify the optimal cost and risk-informed design or maintenance of a system under the single- (e.g., earthquake (Zhu, B. and Frangopol, D. M., 2013; Gomez, C. and Baker, J. W., 2019; Xu, N. *et al*., 2007), hurricane (Mondoro, A. *et al*., 2017), extreme weather (Rocchetta, R. *et al*., 2015) and multihazard conditions (Nikellis, A. and Sett, K., 2020; Chandrasekaran, S. and Banerjee, S., 2016). Often, to optimize the retrofitting of the system (e.g., building (Liu, M. *et al*., 2005), bridge (Kwag, S. and Ok, S. Y., 2013), transportation network (Choi, E. and Song, J.,2019) and power grid (Choi, E. and Song, J., 2020)), multi-objective genetic algorithm (MOGA) is combined with the system-level functionality, reliability, risk, and life cycle cost analysis.

Especially in the nuclear safety engineering domain, the optimal seismic capacity of SSCs of NPP had been studied with consideration of both cost and seismic risk in the work of Kwag and Hahm (2020) and Bolisetti *et al*. (2021). It is identified in these works that optimal relocation of SSCs can reduce both core-damage frequency (CDF) and capital cost more than the original setting. However, the optimal multihazard capacity of NPP which accounting both cost and multihazard risk is not investigated yet. This may be due to the high computational cost for both multihazard risk quantification and optimization algorithm, and the lack of a publicly open capital cost database for the NPP SSCs.

Therefore, to address this computational efficiency issue, we propose a framework that combines MOGA with the two-stage direct quantification of fault tree using Monte Carlo simulation (two-stage DQFM) (Choi *et al*., 2021), which is recently developed by the authors. Also, to resolve the cost data availability issue, we proposed the multihazard cost function which uses the hazard capacity of two hazards indirect measure. In addition, to merge the capital cost for two different hazards, the current budget ratio between the two hazards is also adopted. The proposed methods are demonstrated and tested by a numerical example.

2. MULTIHAZARD RISK QUANTIFICATION OF NPP

While identifying the optimal multihazard capacity of NPP, it is essential to evaluate the multihazard risk as one of the multi-objectives. For multihazard risk quantification of NPP, several methods including Boolean (Leverenz, F. L. and Kirch, H.,1976), Original DQFM (Watanabe, Y. *et al*., 2003), Improved DQFM (I-DQFM) (Kwag, S. *et al*., 2019), and Two-stage DQFM (Choi *et al*., 2021) are developed. Among the proposed sampling-based multihazard risk quantification methods, two-stage DQFM, which was recently developed by the authors, shows a superior outcome in terms of efficiency and accuracy. Therefore, we adopted a two-stage DQFM as a multihazard risk quantification module of the proposed framework. In this section, we briefly summarize the basic idea of conventional DQFM and two-stage DQFM.

2.1. Basic idea of conventional DQFM

Two-stage DQFM uses conventional DQFM as the base algorithm. The algorithm requires a system model (i.e., fault tree), fragility curve of each component, and hazard curve as an input, and begins with setting discrete multi-hazard grids into the uniform interval. For each hazard condition point, the hazard response R and the capacity of the components C are sampled. Both R and C are assumed to be log-normal distributions, which can be expressed as follows:

$$R(a) \sim LN(R_m(a), \beta_{Rc}) \quad (1)$$

$$C(a) \sim LN(C_m(a), \beta_{Cc}) \quad (2)$$

where, LN(α, β) represent the log-normal distribution with median α and log-standard deviation β. β_{Rc} and β_{Cc} denote the composite log-standard deviations of R and C, respectively. While generating R and C for each hazards, partial

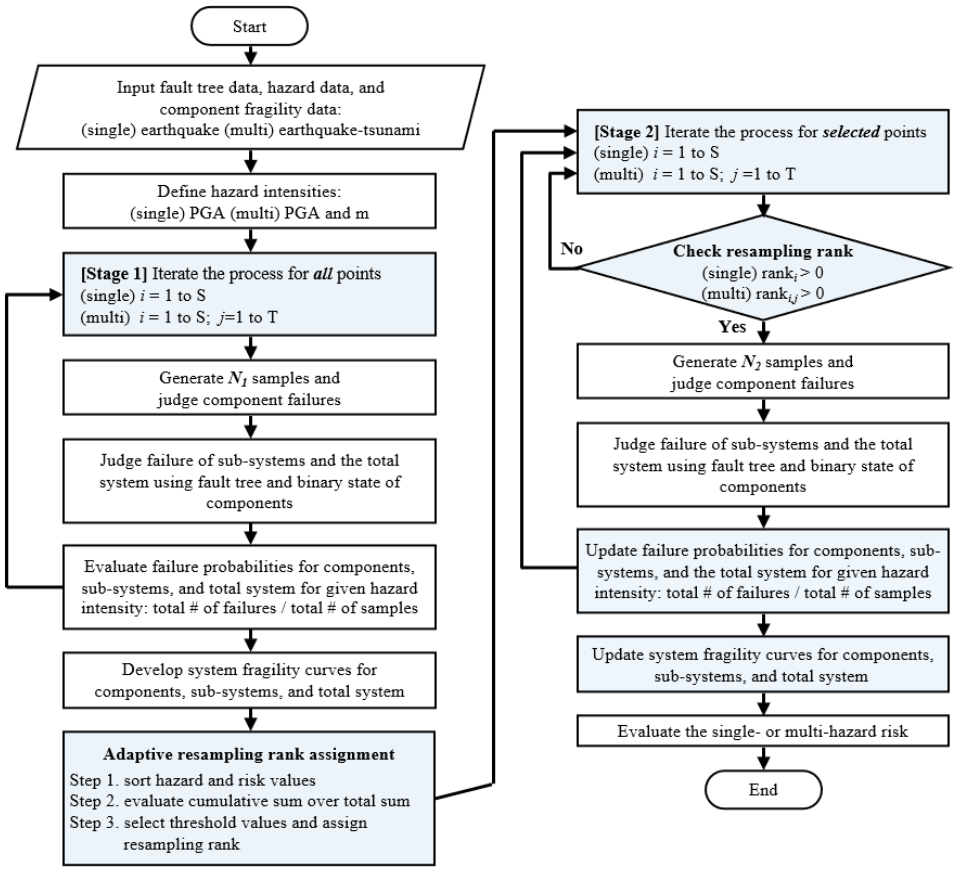

Figure 1: Flowchart of the two-stage DQFM (adopted from Choi et al., 2021).

correlations between the components can be introduced by the correlation coefficient matrix. The generated sample set of *R* and *C* are compared with each other and expressed in binary form (i.e., 0 and 1 represent the survival and failure of the components, respectively). The state of the component is considered as survival only when the component survived both hazards. Using the binary condition of each component and the fault tree, the binary state of the system is decided. The final system fragility is estimated as the number of system failures over the total number of samples N at each multihazard condition (Kwag., 2019).

2.2. Two-stage DQFM

It is important to note that conventional DQFM uses a uniform interval to define hazard conditions, and used a large number of sampling (N = 10^4) for all hazard points. When the contribution of certain multihazard is trivial to the final risk, however, the system failure estimated by small N_1 and large N_2 can have negligible differences. With this inspiration, in the two-stage DQFM, the algorithm generates a relatively small N_1 (e.g., 10^2) sample set for multihazard points that make a little contribution to the final multihazard risk, and generates large enough N_2 (e.g., 10^4) sample set for others (Figure 1).

In the first DQFM stage, a system failure probability is determined for all multihazard points with a small N_1. Using the results of the first DQFM stage, the importance of each multihazard point is identified in terms of its contribution to the final risk. The cumulative ratio of hazard and risk is adopted as the criteria for selecting the resampling points. The cumulative rate of the hazard and risk values for each multihazard point can be determined as follows:

$$H_c(a) = \sum_{i^*=1}^{a} dH(i^*)/dpdq \Big/ \sum_{i^*=1}^{max} dH(i^*)/dpdq \qquad (3)$$

$$R_c(a) = \sum_{i^*=1}^{a} Risk(i^*) \Big/ \sum_{i_S=1}^{max} Risk(i^*) \quad (4)$$

where H_c and R_c are the cumulative rates of the differential hazard values for hazard and risk values, respectively. i^* is the newly given order that was achieved through the min-to-max sorting process. For instance, in previous work on two-stage DQFM, the H3.5R20 threshold, which skip the group of the point that contributed $10^{-3.5}$ to the total differential value of the hazard and those contributed 20% to the final risk value at the second DQFM stage, is identified as a most efficient threshold for multihazard risk evaluation (Choi *et al*., 2021). With these threshold values, multihazard points that are identified to have a non-negligible contribution to the final risk are sampled again at the second DQFM stage with large N_2. Finally, the multihazard risk of the NPP system is determined by a convolution of the hazard curve and the updated fragility curve.

3. MULTIHAZARD CAPACITY OPTIMIZATION OF NPP

3.1. NSGA-II

For the system optimization problems, authors employ the NSGA-II (Deb *et al*., 2002) to optimize the multihazard capacity of SSCs of NPP with two objectives (i.e., multihazard risk and capital cost).

As a bio-inspired optimization algorithm, the NSGA-II algorithm generates the sample population from the initial sample population while pursuing the balance between elitism and exploration. From an initial population, an offspring sample set is generated using the genetic operators (i.e., crossover and random mutation). In this stage, the total sample population is temporarily doubled. To generate the following sample population that is better fitted to the selected objective functions, the fitness of each sample is evaluated for both parents and offspring populations. In this step, the multihazard risk is evaluated using two-stage DQFM (light blue colored in Figure 2) as one of the objectives.

Later, using the objective values of the sample population, the Pareto rank is assigned using fast non-dominated sorting and crowd distance sorting. With these criteria, eventually, the sample sets more- fitted to the objective functions and more spread in search space are chosen as the parent sample of the following generation.

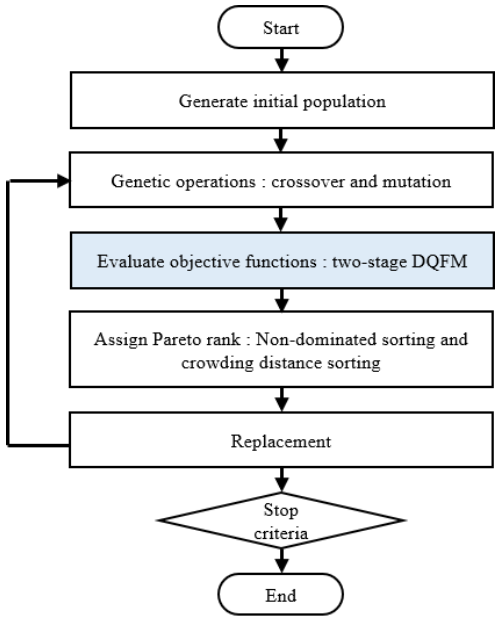

Figure 2. Flowchart of the NSGA-II

3.2. Genetic representation

To optimize the multihazard capacity of the NPP using a genetic algorithm-based method, multihazard capacity requires a genetic representation. As illustrated in Figure 3, we propose a polynomial string that represents the multihazard capacities. The length of the string can be varying by the type of multihazard combination.

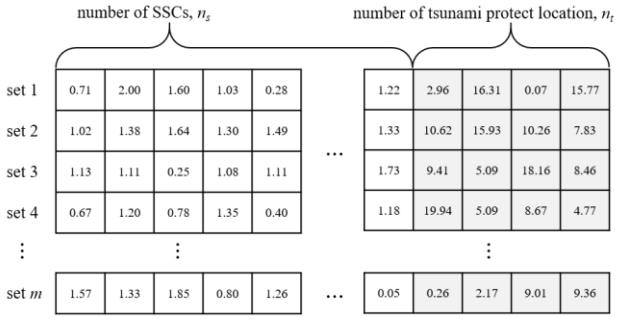

Figure 3. Genetic representation of earthquake-tsunami hazard capacity of NPP

3.3. Multi-objective functions

To identify the optimal multihazard capacity of the NPP in terms of both multihazard risk and capital cost, two objective functions which generally have a trade-off relationship are selected: (1) multihazard risk of NPP, and (2) capital cost.

3.3.1. Multihazard risk: core damage frequency

The CDF under multihazard condition is adopted as the objective function to identify the multihazard capacity setting that reduces the multihazard risk. The CDF can be described as:

$$Risk_{multi} = \int_0^\infty \cdots \int_0^\infty F(p, \cdots, q) \frac{dH(p, \cdots q)}{dp \cdots dq} dp \cdots dq \qquad (3)$$

where p and q denote multihazard intensity and F and H are the system failure probability multihazard curve, respectively. Since we pursue to reduce the multihazard CDF of current NPP, risk measure is normalized by dividing the CDF of sample NPP by those of current NPP.

3.3.2. Multihazard capital cost

To identify the optimal multihazard capacity also in terms of the capital cost, measuring the capital cost of a given multihazard setting of NPP is important. If the capital cost database is available, and the relationship between the SSCs capacity and cost is given, the total capital cost for NPP can be estimated from those models. However, it is difficult to apply for most multihazards, since monetary cost data of the NPP design against the hazards are publicly not available. Therefore, under the assumption that capital cost is proportional to each hazard capacity (Kwag and Hahm (2020), an indirect capacity-based cost model is proposed in this paper as follows:

$$Cost_{multi} = \frac{1}{1+\alpha}\left(\frac{\sum A_{m1_i}}{\sum A'_{m1_i}} + \alpha \frac{\sum A_{m2_j}}{\sum A'_{m2_j}}\right) \qquad (4)$$

where A_{m1} and A_{m2} denotes the median capacity of sample set for hazard 1 and 2, respectively. $A'm$ is the median capacity of current NPP. In addition, to combine the cost of two different hazards in one measure, the current budget ratio between the two hazard capacities α is adopted as weighting factor. If current cost for hazard 2 capacity is double the those of hazard 1 capacity, value of α is 2. In addition, proposed cost measure is normalized by the current multihazard capacity of NPP.

4. NUMERICAL EXAMPLES

4.1. Problem setting

To illustrate the proposed framework and to investigate the effect of the parameters (i.e., the ratio between seismic and tsunami capacity cost), a multi-hazard example, the NPP under earthquake–tsunami hazard was investigated. The earthquake–tsunami hazard information was taken from a report by the Korea Atomic Energy Research Institute (KAERI, 2017) and the NPP system model and component multihazard information is adapted from the work of Ellingwood (1990) and Kwag *et al*. (2019). The NPP system core meltdown (CM) model is described in Eqs. 5 to 6, respectively. The list of LGS NPP components is summarized in Table 1.

$$A = S_{11} \cup S_{12} \cup S_{13} \cup S_{14} \cup S_{15} \cup S_{16} \cup DG_R \qquad (5)$$

$$CM = S_4 \cup S_6 \cup S_1 \cap [A \cup (S_3 \cup C_R) \cap (S_{10} \cup SLC_R) \cap (S_{17} \cup W_R)] \qquad (6)$$

Among these system components, some are likely to have correlated multihazard response and capacity due to their spatial proximity. Therefore, components S11, S12, S13, and S14 which are located in the same reactor building; and components S15 and S16 located in the same diesel generator building are assumed to be partially correlated ($\rho_s = \rho_t = 0.7$).

These spatial distributions of the SSCs also affect the genetic representation of the multihazard capacity of SSCs. Under the assumption that the seismic capacity of SSCs can be chosen for each component while the tsunami protection is assigned for each location, a string with a length of 18 (sum of n_s 13 and n_t 5) is chosen as a genetic representation of multihazard

capacity of NPP. In the string, the first 13 values indicate the median seismic capacity of SSCs components from S1 to S17, and the following values represent the median tsunami capacity of Offsite (S1), Condensate storage tank (S2), Reactor building (S11, S12, S13, and S14), Diesel generator circuit (S15), and RHR heat exchangers (S17).

Table 1: LGS NPP components

Components			
S_1	*Offsite power*	S_{14}	*4-kV bus / steam generator*
S_2	*Condensate storage tank*	S_{15}	*Diesel generator circuit*
S_3	*Reactor internals*	S_{16}	*Diesel generator heat and vent*
S_4	*Reactor enclosure structure*	S_{17}	*Residual heat removal system heat exchangers*
S_6	*Reactor pressure vessel*	DG_R	*DGR – diesel generator common mode*
S_{10}	*Standby liquid control system tank*	W_R	*WR – containment heat removal*
S_{11}	*440-V bus / steam generator breakers*	C_R	*CR – scram system mechanical failure*
S_{12}	*440-V bus transformer breaker*	SLC_R	*SLCR – standby liquid control*
S_{13}	*125/250-V DC bus*		

Finally, the current cost ratio between the seismic and tsunami capacity budget α and the capacity limits for seismic and tsunami capacity should be also selected to perform the optimization. The parametric study is performed with seven values (i.e., α = 0, 0.25, 0.5, 1, 2, 4, and infinite), and their effect on final Pareto solutions are compared with each other.

Besides the multihazard budget ratio α and capacity constraints, various parameters should be selected to perform the prosed method. First, while performing two-stage DQFM, the seismic intensity (PGA, g) and tsunami intensity (inundation depth, m) were uniformly divided into 21 and 41 points, respectively. Also, the H3.5R20 threshold is chosen (Choi *et al*., 2021), and the number of samples 10^2 and 10^4 are used for the first and second stages of two-stage DQFM, respectively. Second, for the NSGA-II, the population size is 100; the mutation ratio is 1/18 (Ochoa, G., 2002); the number of total generations 1200 is conservatively determined based on several test runs.

4.2. Results and discussions

Figure 4 shows the Pareto solutions of multihazard capacity relocation of NPP with seven different earthquakes and tsunami capacity budget of the current NPP and the critical zone (shaded area). The optimal system curves of NPP and the detail distribution of the multihazard capacity of each SSCs are investigated for default setting (i.e., α = 1; seismic and tsunami capacity range from 0g to 3g and from 0 m to 20m, respectively) (black line in Figure 4). These upper limits are selected to provide sufficient search space to the algorithm, and not to limit the potential optimal solutions by selected constraints.

Each point that constructs the Pareto curve indicates the certain non-dominated optimal NPP SSCs solutions. Figure 5 shows the multihazard fragility of NPP at the system level, some of the non-dominated optimal solutions ("o" marks in figure 4) are compared with the original NPP conditions. For instance, the red curve indicated the system fragility curve that delivers the same multihazard CM value with only 24.5% of the current NPP cost. While its system failure probability has a negligible difference in most hazard conditions, shows lower system failure probability at relatively low PGA and high tsunami height conditions. On the other hand, the cyan-colored curve indicated the system fragility curve that reduces 20% of both the current NPP cost and CM risk; and blue colored curve indicated the system fragility curve that maintains the current NPP cost and reduces 24.2% of the current NPP cost and reduces 24.2% of the current NPP CM risk.

Relocating optimal capacity for each SSCs on a given budget cannot be directly known by intuition, and become further challenging as the system model become more complex system size increases and the number of hazard increases. In these circumstances, the proposed method successfully identifies the group of non-dominated solutions with consideration of cost and multihazard risk and therefore will provide useful insight to the management authorities who aim to reduce both multihazard risk and cost of current NPP by SSCs capacity relocation.

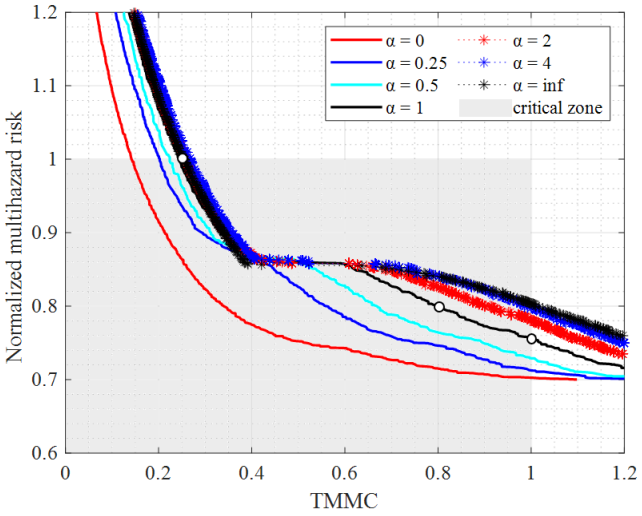

Figure 4. Pareto solutions of multihazard capacity relocation of NPP with various α

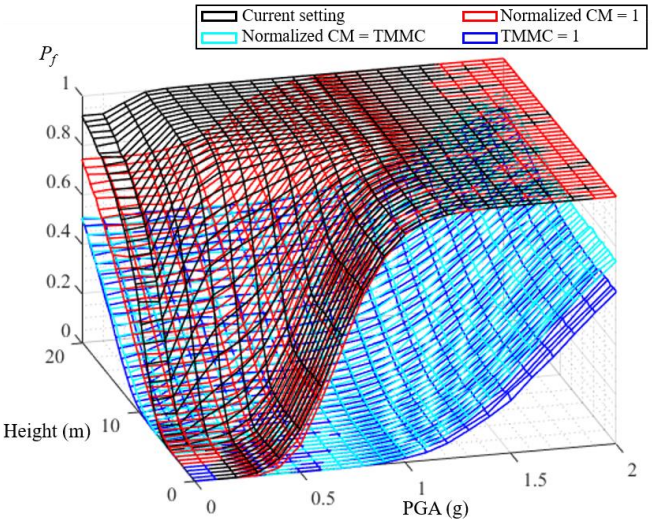

Figure 5. Comparison of the optimal system fragility curves with current NPP ("o" marks in figure 5)

5. CONCLUSIONS

In this study, a multihazard capacity optimization framework that combines NSGA-II and two-stage DQFM is proposed for NPP SSCs. To perform optimization, the genetic representation of the multihazard capacity of NPP SSCs, and the indirect cost measure were also proposed. Through the numerical example, it is identified the proposed framework and objective functions successfully identify the optimal SSCs multihazard capacity setting which accounting both multihazard risk and cost. We expect that the proposed method can provide useful insight to the NPP management authorities by demonstrating a group of optimal system settings that can reduce both multihazard risk and corresponding capital cost.

ACKNOWLEDGMENTS

This study was supported by the National Research Foundation of Korea (NRF) grant funded by the Korea government (Ministry of Science and ICT) (No. RS-2022-00154571).

6. REFERENCES

Bolisetti, C., Coleman, J., Hoffman, W., &Whittaker, A. (2021). Cost-and Risk-Based Seismic Design Optimization of Nuclear Power Plant Safety Systems. Nuclear Technology, 207(11), 1687-1711.

Chandrasekaran, S., & Banerjee, S. (2016). Retrofit optimization for resilience enhancement of bridges under multihazard scenario. Journal of Structural Engineering, 142(8), C4015012.s

Choi, E., & Song, J. Development of Multi-Group Non-dominated Sorting Genetic Algorithm for identifying critical post-disaster scenarios of lifeline networks. International Journal of Disaster Risk Reduction 41 (2019) 101299.

Choi, E., Ha, J., Hahm, D., and Kim, M. A Review of Multihazard Risk Assessment: Progress, Potential, and Challenges in the Application to Nuclear Power Plants. International Journal of Disaster Risk Reduction 53 (2020) 101933.

Choi, E., & Song, J. Cost-effective retrofits of power grids based on critical cascading failure scenarios identified by multi-group non-dominated sorting genetic algorithm.

International Journal of Disaster Risk Reduction 49 (2020) 101640.

Choi, E., Kwag, S., Ha, J., Hahm, D., Development of a Two-stage DQFM for Efficient Single- and Multi-hazard Risk Quantification for Nuclear Facilities. Energies 14(4) (2021) 1017.

Deb, K., Pratap, A., Agarwal, S., and Meyarivan, T. A. M. T. A fast and elitist multiobjective genetic algorithm: NSGA-II. IEEE transactions on evolutionary computation 6.2 (2002): 182-197.

Ellingwood, B. Validation studies of seismic PRAs. Nuclear Engineering and Design 123 (1990) 189-196.

Gomez, C., & Baker, J. W. (2019). An optimization-based decision support framework for coupled pre-and post-earthquake infrastructure risk management. Structural Safety, 77, 1-9.

KAERI. Development of Site Risk Assessment & Management Technology including Extreme External Events. KAERI/RR-4225/2016, Korea Atomic Energy Research Institute, Daejeon, South Korea (2017).

Kwag, S., & Ok, S. Y. (2013). Robust design of seismic isolation system using constrained multi-objective optimization technique. KSCE Journal of Civil Engineering, 17(5), 1051-1063.

Kwag, S., Ha, J. G., Kim, M. K., & Kim, J. H. Development of Efficient External Multi-Hazard Risk Quantification Methodology for Nuclear Facilities. Energies 12(20) (2019) 3925.

Kwag, S., &Hahm, D. (2020). Multi-objective-based seismic fragility relocation for a Korean nuclear power plant. Natural Hazards, 103(3),3633-3659.

Leverenz, F. L., & Kirch, H. (1976). User's guide for the WAM-BAM computer code (No. PB--249624). Science Applications. Inc., Palo Alto, CA., USA.

Liu, M., Burns, S. A., & Wen, Y. K. (2005). Multiobjective optimization for performance-based seismic design of steel moment frame structures. Earthquake Engineering & Structural Dynamics, 34 (3), 289-306.

Mondoro, A., Frangopol, D. M., & Soliman, M. (2017). Optimal risk-based management of coastal bridges vulnerable to hurricanes. Journal of Infrastructure Systems, 23(3), 04016046.

Nikellis, A., & Sett, K. (2020). Multihazard Risk Assessment and Cost-Benefit Analysis of a Bridge-Roadway-Levee System. Journal of Structural Engineering, 146(5), 04020050.

Ochoa, G. Setting the mutation rate: Scope and limitations of the 1/L heuristic. Proceedings of the 4th Annual Conference on Genetic and Evolutionary Computation. Morgan Kaufmann Publishers Inc., (2002).

Rocchetta, R., Li, Y., & Zio, E. (2015). Risk assessment and risk-cost optimization of distributed power generation systems considering extreme weather conditions. Reliability Engineering & System Safety, 136, 47-61.

Watanabe, Y., Oikawa, T., & Muramatsu, K. (2003). Development of the DQFM method to consider the effect of correlation of component failures in seismic PSA of nuclear power plant. Reliability Engineering & System Safety, 79(3), 265-279.

Xu, N., Davidson, R. A., Nozick, L. K., & Dodo, A. (2007). The risk-return tradeoff in optimizing regional earthquake mitigation investment. Structure and Infrastructure Engineering, 3(2), 133-146.

Zhu, B., & Frangopol, D. M. (2013). Risk-based approach for optimum maintenance of bridges under traffic and earthquake loads. Journal of structural engineering, 139(3), 422-434.